orbital. The latter is strongly antibonding with respect to the quinone C–O bonds, and it has a significant contribution from the oxygen $2p_z$ orbital. However, oxygen-bound quinones are not usually π acceptors but rather oxidizing ligands whose complete reduction alters significantly both their electronic and molecular structure[11,28,31] and strengthens also their bonding to the central metal atom.[11] This $d_\pi \rightarrow \pi^*$(LUMO) electron transfer concerted with the formation of a Cr–O(quinone) σ bond may thus be regarded as a net electron transfer in accordance with the formulation of the addition of *o*-quinones as an oxidative addition (eq 8).

The photochemical formation of $\mathrm{Cr(SQ)_3}$ complexes represent the first well-characterized example of photochemical oxidative substitution of group VIB metal carbonyls in solution. However, this process might be of more general and practical importance as is shown e.g. by polymerizations photosensitized by various metal carbonyls in the presence of $\mathrm{CCl_4}$.[32] These processes seem to be initiated by various radicals formed in the photoredox reactions of $\mathrm{CCl_4}$ with metal carbonyls (including $\mathrm{Cr(CO)_6}$). Our preliminary results show formation of $\mathrm{CrCl_3}$ when $\mathrm{Cr(CO)_6}$ is irradiated in pure $\mathrm{CCl_4}$.

Analogously $\mathrm{Cr_2O_3}$ is slowly formed by an oxidative substitution of $[\mathrm{Cr(CO)_5(CH_3CN)}]$ in the presence of dioxygen.[33] Recent low- temperature matrix isolation studies[34,35] show the formation of mixed-carbonyl–oxygen complexes by the photochemical reaction of $\mathrm{M(CO)_6}$ (M = Cr, Mo, W) with dioxygen at 10 K.

Moreover, a number of very slow thermal reactions between group VIB metal carbonyls and oxidizing substrates, producing M(III) complexes, has been described.[36-38] Compounds containing active reducible protons (β-diketonates, carboxylic acids, or Schiff bases)[36,37] and also compounds containing S–S bonds[38] were employed as oxidizing substrates. Some of these synthetic reactions were also recently carried out photochemically.[39]

It might thus be argued that photochemical oxidative substitutions of group VIB metal carbonyls represent a more general class of processes that may be widely used in synthesis and, perspectively, in photocatalysis, especially in the case of Mo and W carbonyls, where low-valent mixed-carbonyl–ligand complexes may be expected to be produced by the irradiation of $\mathrm{Mo(CO)_6}$ or $\mathrm{W(CO)_6}$ with suitable oxidizing substrates at ambient or low temperatures.

Acknowledgment. I am indepted to Ing. A. Fojtík, C.Sc., for his kind technical assistance in flash photolytic measurements.

Registry No. $\mathrm{Cr(CO)_6}$, 13007-92-6; CQ, 2435-53-2; DBQ, 3383-21-9; $\mathrm{Cr(CO)_5}$, 26319-33-5; $\mathrm{Cr(DBSQ)_3}$, 64020-84-4; PQ, 84-11-7.

---

(31) Vlček, A., Jr.; Klíma, J.; Vlček, A. A. *Inorg. Chim. Acta* **1982**, *58*, 75.

(32) Balzani, V.; Carassiti, V. "Photochemistry of Coordination Compounds"; Academic Press: New York, 1970.

(33) Strohmeier, W.; Gerlach, K. *Z. Naturforsch., B: Anorg. Chem., Org. Chem., Biochem., Biophys., Biol.* **1960**, *15B*, 622.

(34) Poliakoff, M.; Smith, K. P.; Turner, J. J.; Wilkinson, A. J. *J. Chem. Soc., Dalton Trans.* **1982**, 651.

(35) Crayston, J. A.; Almond, M. J.; Downs, A. J.; Poliakoff, M.; Turner, J. J. *Inorg. Chem.* **1984**, *23*, 3051.

(36) Dunne, T. G.; Cotton, F. A. *Inorg. Chem.* **1963**, *2*, 263.

(37) Calderazzo, F.; Floriani, C.; Henzi, R.; L'Eplattenier, F. *J. Chem. Soc. A* **1969**, 1378.

(38) Davison, A.; Edelstein, N.; Holm, R. H.; Maki, A. H. *J. Am. Chem. Soc.* **1964**, *86*, 2799.

(39) Thomas, P.; Schreckenbach, J.; Hennig, H. *Z. Chem.* **1984**, *24*, 413.

(40) Downs, H. H.; Buchanan, R. M.; Pierpont, C. G. *Inorg. Chem.* **1979**, *18*, 1736.

(41) Gordon, D. J.; Fenske, R. F. *Inorg. Chem.* **1982**, *21*, 2907.

(42) The periodic group notation in parentheses is in accord with recent actions by IUPAC and ACS nomenclature committees. A and B notation is eliminated because of wide confusion. Groups IA and IIA become groups 1 and 2. The d-transition elements comprise groups 3 through 12, and the p-block elements comprise groups 13 through 18. (Note that the former Roman number designation is preserved in the last digit of the new numbering: e.g., III → 3 and 13.)

Contribution from the Department of Chemistry,
Massachusetts Institute of Technology, Cambridge, Massachusetts 02139

Resonance Raman Spectroscopy of the Lowest Excited State of Derivatives of Tris(2,2′-bipyridine)ruthenium(II): Substituent Effects on Electron Localization in Mixed-Ligand Complexes

Patricia A. Mabrouk and Mark S. Wrighton*

Received June 17, 1985

The one-electron nature of the lowest electronic excited state of $[\mathrm{RuL}_n\mathrm{L'}_{3-n}]^{2+}$ (L, L′ = 2,2′-bipyridine (bpy), 4,4′-dimethyl-2,2′-bipyridine ($\mathrm{Me_2bpy}$), 4,4′-dibromo-2,2′-bipyridine ($\mathrm{Br_2bpy}$); n = 0, 1, 2, 3) as the $\mathrm{PF_6^-}$ salts in $\mathrm{CH_3CN}$ at 25 °C has been investigated by optical absorption and emission spectral studies and by resonance Raman spectroscopy. For the Raman studies, a high concentration of excited species was produced by the leading edge of a frequency-tripled Nd:YAG laser pulse (~18 ns; 354.7 nm; ~3 mJ) and the Raman scattering from the trailing edge of the pulse was monitored. For all $[\mathrm{RuL_3}]^{2+}$ species the data are interpreted as revealing a lowest excited state that has the excited electron localized on one of the three equivalent ligands, as previously established for $[\mathrm{Ru(bpy)_3}]^{2+}$. Generally, for the mixed-ligand complexes the excited electron is localized on the more easily reduced ligand, on the time scale of the probe (~18 ns). However, the complexes $[\mathrm{Ru(bpy)(Me_2bpy)_2}]^{2+}$ and $[\mathrm{Ru(bpy)_2(Br_2bpy)}]^{2+}$ show excited-state Raman spectra consistent with a mixture of excited species, only a fraction with the excited electron localized on the more easily reduced ligand. Optical emission spectra show that substituent effects can be important, even though the substituent variation occurs in a ligand that is not the ligand on which the excited electron is localized. For example, $[\mathrm{Ru(bpy)(Me_2bpy)_2}]^{2+}$ emits at lower energy (~450 $\mathrm{cm^{-1}}$) than $[\mathrm{Ru(bpy)_3}]^{2+}$, though both excited species involve an excited electron localized on the 2,2′-bipyridine ligand. The lower energy excited state is due to the destabilization of the d-π(HOMO) orbital in the ground-state 4,4′-dimethyl-2,2′-bipyridine species. Consistent with such an interpretation, the $E°'$ for the $[\mathrm{Ru(Me_2bpy)_3}]^{3+/2+}$ redox couple is ~0.2 V negative of that for the 2,2′-bipyridine analogue.

In this paper we present new information concerning ligand substituent effects on the electron distribution in the lowest electronic excited state of $[\mathrm{Ru(bpy)_3}]^{2+}$. In particular, we demonstrate that the mixed-ligand complexes $[\mathrm{RuL}_n\mathrm{L'}_{3-n}]^{2+}$ (L, L′ = 2,2′-bipyridine (bpy), 4,4′-dimethyl-2,2′-bipyridine ($\mathrm{Me_2bpy}$), 4,4′-dibromo-2,2′-bipyridine ($\mathrm{Br_2bpy}$); n = 0, 1, 2, 3) can be probed by excited-state Raman spectroscopy. This work was undertaken to establish the effect of substituents in directing the extent of electron localization on a given ligand and to assess the substituent effect on the excited-state energy.

The lowest $[\mathrm{Ru(bpy)_3}]^{2+}$ excited state is Ru → π^*(bpy) charge transfer (MLCT) in character and has been well established as such.[1-6] The excited state can be viewed, in the one-electron

---

* To whom correspondence should be addressed.

0020-1669/86/1325-0526$01.50/0 © 1986 American Chemical Society

extreme, as a complex of Ru(III), $[L_2Ru^{III}L^-]^{2+}$. This view is supported by transient-absorption[6] and Raman spectra of the excited species.[7] The spectra closely resemble those for L^-, L = 2,2′-bipyridine. A priori, the introduction of substituents in an asymmetrical fashion can stabilize the excited Ru(II) complex. To illustrate, electron-releasing substituents on two of the bpy ligands should yield a lower energy excited species with the excited electron localized on the remaining bpy ligand. We now report spectroscopic and electrochemical findings for the $[RuL_3]^{2+}$ (L = bpy, Me_2bpy, Br_2bpy) and the mixed-ligand $[RuL_nL'_{3-n}]^{2+}$ complexes to demonstrate that such excited-state stabilization can be achieved. Understanding the behavior of mixed-ligand complexes is likely to be crucial in developing the ability to control excited-state electron transfer in organized assemblies for conversion of optical energy.[8]

Experimental Section

Optical Absorption and Emission Spectral Measurements. UV/vis spectra of complexes were recorded at room temperature for $\sim 10^{-4}$ M solutions on a Cary 17 UV/vis/near-IR spectrophotometer. Emission spectra were obtained on a Hitachi/Perkin-Elmer MPF 44 spectrophotometer. All emission spectra were recorded for 10^{-4} M (deoxygenated) CH_3CN or CH_2Cl_2 solutions. The samples were typically deoxygenated by purging with pure N_2 gas. A slit width of 10 nm was used for both excitation and emission monochromators.

Infrared Spectral Measurements. IR spectra at 2-cm^{-1} resolution of $[fac\text{-}(CH_3CN)Re(CO)_3L][CF_3SO_3]$ complexes (L = bpy, Me_2bpy, Br_2bpy) were recorded at room temperature in CH_3CN on a Perkin-Elmer 180 spectrometer.

Electrochemistry. Electrochemical measurements were made with a PAR Model 173 potentiostiat and a Model 175 Universal Programmer. Cyclic voltammograms were recorded with a Houston Instruments Model 2000 X-Y recorder. Measurements were made on $\sim 10^{-3}$ M solutions using freshly distilled, dry CH_3CN as solvent contained in septa-sealed three-neck 50-mL round-bottom flasks. A single junction Ag^+/Ag reference electrode, a Pt-wire working electrode, and a Pt-gauze counter electrode were used in all experiments. The supporting electrolyte was 0.1 M $[n\text{-}Bu_4N]BF_4$. Solutions were N_2-purged for at least 5 min and were used immediately thereafter.

Raman Spectroscopy. Ground-state resonance Raman spectra were recorded on a Spex Ramalog 4 spectrometer. Laser excitation at 457.9 nm with 50–70 mW of power incident at a spinning sample was obtained by using a Coherent CR-2 Ar^+ laser. Slits were set to 100, 150, and 100 μm for 2-cm^{-1} resolution in all spectra. The samples were studied as $\sim 10^{-3}$ M solutions in CH_3CN and were degassed in three freeze–pump–thaw cycles and sealed prior to study. The samples were contained in 5-mm NMR tubes. Raman scattering was monitored at 45° to the laser beam utilizing a backscattering geometry. The 917-cm^{-1} band of CH_3CN was used as an internal standard in all cases. All observed intensities are relative and not true intensities and have not been corrected for the spectral sensitivity of the instrument.

Excited-state Raman spectra were recorded on an instrument previously described.[9] An integration time of 5 min/500-cm^{-1} scan was used for all samples employed in this study. The power incident at the sample was 3 mJ/pulse, and the pulse rate was 10 Hz. Both the 917- and 1372-cm^{-1} Raman bands of CH_3CN were used in the frequency calibration of the excited-state spectra. The resolution of the spectrometer is ~ 10 cm^{-1}. All samples were freeze–pump–thaw degassed in three cycles and sealed immediately prior to study.

Materials. The following materials were obtained commercially and used as received: bpy (MCB); Me_2bpy (G. F. Smith); $RuCl_3$ (Aldrich); $Ru(bpy)_2Cl_2$ (Strem); $AgCF_3SO_3$ and NH_4PF_6 (Alfa). The spectroscopic grade CH_3CN used in all work was distilled from P_2O_5 and stored under dry N_2 prior to use. All other solvents used in the preparative work were obtained commercially and used without further purification.

Preparation of 4,4′-Dibromo-2,2′-bipyridine. This ligand was prepared by using the method of Maerker and Case.[10] However, in our work the $CHCl_3$ phase was evaporated in vacuo sufficiently as to cause precipitation of the fluffy white product. This material was recrystallized once from Et_2O, purified by sublimation, and further purified by chromatography on a 1 × 20 cm column of activated Al_2O_3. The eluent was CCl_4. The yield was 68%. Identification of the compound was established by ^1H NMR. ^1H NMR (JEOL 90-MHz Fourier transform) (acetone-d_6): δ 8.61 (d, 2 H, J = 1.0 Hz), 8.56 (s, 1 H), 7.74 (d, 1 H, J = 1.0 Hz), 7.68 (d, 2 H, J = 1.0 Hz).

General Preparation of $RuL_2Cl_2 \cdot 2H_2O$ (L = 4,4′-Me_2bpy, 4,4′-Br_2bpy).[11] The method is outlined for $Ru(Me_2bpy)_2Cl_2 \cdot 2H_2O$. Commercial $RuCl_3$ (7.6 mmol), Me_2bpy (16.3 mmol), and LiCl (1.0 mmol) were refluxed for 8 h under N_2 in 20 mL of dimethylformamide. During this time the mixture was magnetically stirred. The solution was reduced to approximately one-third volume, and 100 mL of acetone was added. The solution was then set aside for 4–5 h in an ice/H_2O bath. The product was precipitated as fine red-black crystals, which were washed with a generous amount of ice-cold H_2O followed by cold Et_2O and dried by suction. The yield was 72%. The method of synthesis for the analogous Br_2bpy complex is similar.

General Preparation of $[RuL_2L'][PF_6]_2$ (L, L′ = bpy, Me_2bpy, Br_2bpy).[11] The method is detailed for the synthesis of $[Ru(bpy)(Me_2bpy)_2][PF_6]_2$. $Ru(Me_2bpy)_2Cl_2 \cdot 2H_2O$ (0.86 mmol) and bpy (6.4 mmol) were refluxed overnight under N_2 in 30–50 mL of C_2H_5OH. The mixture was magnetically stirred throughout this period. An excess of NH_4PF_6 was added, and the mixture was then set aside to cool to room temperature. The flask was placed in an ice/H_2O bath for 2–3 h to promote more complete precipitation of the crude product. Final purification of the complex was then carried out by slow recrystallization from acetone/Et_2O. The red product was washed with ice-cold H_2O and Et_2O and dried by suction. The yield was 86%. Similar procedures were used to prepare the other complexes.

General Preparation of $[RuL_3][PF_6]_2$ (L = bpy, Me_2bpy, Br_2bpy).[11] The method is outlined for the synthesis of $[Ru(Me_2bpy)_3][PF_6]_2$. Commercial $RuCl_3$ (2.6 mmol) and Me_2bpy (16.3 mmol) were refluxed overnight in 100 mL of C_2H_5OH under Ar. Throughout this period the reaction mixture was magnetically stirred. An excess of NH_4PF_6 was added to the still warm solution, and the mixture was set aside to cool. The flask was then placed in an ice/H_2O bath for several hours to effect more complete precipitation of the product. The crude product was slowly recrystallized to yield brick red crystals. The yield was 55%. A similar method may be used to prepare the other complexes.

General Preparation of $[fac\text{-}(CH_3CN)Re(CO)_3L][CF_3SO_3]$ (L = bpy, Me_2bpy, Br_2bpy). The $[(CH_3CN)Re(CO)_3phen]Tf$ (Tf = $CF_3SO_3^-$) complex has been synthesized and reported in the literature.[12] Synthesis of the analogous bpy complexes was carried out in a similar manner and is outlined for the preparation of $[fac\text{-}(CH_3CN)Re(CO)_3bpy]Tf$. The precursor $ClRe(CO)_3L$ complexes were prepared by reaction of $ClRe(CO)_5$ with L.[12] $ClRe(CO)_3bpy$ (1.1 mmol) and AgTf (~ 2 mmol) were placed in a 250-mL round-bottom flask and dissolved with approximately 100 mL of CH_3CN. This mixture was then refluxed overnight under N_2 with stirring. As the reaction proceeded AgCl precipitated on the walls of the flask. At the end of the reaction period the solution was suction-filtered to remove AgCl and then reduced to dryness. A minimal quantity of fresh CH_3CN was added to dissolve the product, and the solution was gently agitated. The material not dissolved is starting material and was removed by filtration. The filtered solution was reduced to half volume, and dry Et_2O was added dropwise (~ 50 mL) until the solution appeared cloudy. The septum-capped solution was placed in the refrigerator overnight to complete precipitation of the product. The product precipitated as golden needles. The yield was 50%.

Results and Discussion

Optical Absorption and Emission Spectra of $[RuL_nL'_{3-n}]^{2+}$ Complexes. Like $[Ru(bpy)_3]^{2+}$,[13] the various complexes syn-

---

(1) Balzani, V.; Bolletta, F.; Gandolfi, M. T.; Maestri, M. *Top. Curr. Chem.* **1978**, *75*, 1.

(2) Meyer, T. J. *Acc. Chem. Res.* **1978**, *11*, 94.

(3) Meyer, T. J. *Prog. Inorg. Chem.* **1983**, *30*, 389.

(4) Watts, R. J. *J. Chem. Educ.* **1983**, *60*, 834.

(5) Watts, R. J.; Harrington, J. S.; Van Houten, J. *Adv. Chem. Ser.* **1978**, *No. 168*, 57.

(6) (a) Bensasson, R.; Salet, C.; Balzani, V. *J. Am. Chem. Soc.* **1976**, *98*, 3722. (b) Sutin, N.; Creutz, C. *Adv. Chem. Ser.* **1978**, *No. 168*, 1.

(7) (a) Dallinger, R. F.; Woodruff, W. H. *J. Am. Chem. Soc.* **1979**, *101*, 4391. (b) Bradley, P. G.; Kress, N.; Hornberger, B. A.; Dallinger, R. F.; Woodruff, W. H. *J. Am. Chem. Soc.* **1981**, *103*, 7441. (c) Forster, M.; Hester, R. E. *Chem. Phys. Lett.* **1981**, *81*, 42. (d) Woodruff, W. H.; Dallinger, R. F.; Hoffman, M. Z.; Bradley, P. G.; Presser, D.; Malvey, V.; Kessler, R. J.; Norton, K. A. In "Time-Resolved Vibrational Spectroscopy"; Atkinson, G. H., Ed.; Academic Press: New York, 1983. (e) Smothers, W. K.; Wrighton, M. S. *J. Am. Chem. Soc.* **1983**, *105*, 1067.

(8) Wrighton, M. S. *Comments Inorg. Chem.* **1985**, *4*, 269.

(9) Mabrouk, P. A.; Wrighton, M. S. *Chem. Phys. Lett.* **1984**, *103*, 332.

(10) Maerker, G.; Case, F. H. *J. Am. Chem. Soc.* **1958**, *80*, 2745.

(11) Related compounds have been synthesized: (a) Dwyer, F. P.; Goodwin, H. A.; Gyarfas, E. C. *Aust. J. Chem.* **1963**, *16*, 42. (b) Crosby, G. A.; Elfring, W. H., Jr. *J. Phys. Chem.* **1976**, *80*, 2206. (c) Elliot, C. M.; Hershenhart, E. J. *J. Am. Chem. Soc.* **1982**, *104*, 7519.

(12) Fredricks, S. M.; Luong, J. C.; Wrighton, M. S. *J. Am. Chem. Soc.* **1979**, *101*, 7415.

Table I. Optical Absorption and Emission Data for Relevant Complexes[a]

	abs max		obsd emissn max[b]	
complex	λ, nm	$\epsilon \times 10^{-4}$, M^{-1} cm^{-1} [a]	λ, nm	ν, cm^{-1}
$[Ru(bpy)_3]^{2+}$	443	1.5	608	16450
$[Ru(bpy)_2(Me_2bpy)]^{2+}$	445	1.6	615	16250
$[Ru(bpy)(Me_2bpy)_2]^{2+}$	449	1.4	625	16000
$[Ru(Me_2bpy)_3]^{2+}$	450	1.7	618	16200
$[Ru(bpy)_3]^{2+}$	443	1.5	608	16450
$[Ru(bpy)_2(Br_2bpy)]^{2+}$	450	1.4	647	15450
$[Ru(bpy)(Br_2bpy)_2]^{2+}$	456	1.0	636	15720
$[Ru(Br_2bpy)_3]^{2+}$	456	1.9	624	16000
$[Ru(Me_2bpy)_3]^{2+}$	450	1.7	618	16200
$[Ru(Me_2bpy)_2(Br_2bpy)]^{2+}$	455	1.3	661	15100
$[Ru(Me_2bpy)(Br_2bpy)_2]^{2+}$	452	1.1	647	15450
$[Ru(Br_2bpy)_3]^{2+}$	456	1.9	624	16000
$[(CH_3CN)Re(CO)_3(bpy)]^{+}$ [c]	346	0.3	525	19000
$[(CH_3CN)Re(CO)_3(Me_2bpy)]^{+}$ [c]	336	0.4	516	19400
$[(CH_3CN)Re(CO)_3(Br_2bpy)]^{+}$ [c]	355	0.4	550	18200

[a] Determination of ε based on a single run on a Cary 17 UV/vis/near-IR spectrometer using ~2 × 10^{-4} M solution in CH_3CN. [b] Uncorrected for small variations in sensitivity of detector at different energies. [c] Since the charge-transfer band appears as only a shoulder in CH_3CN, it is difficult to assign absorption maxima. Thus, data for the Re complexes are reported for CH_2Cl_2 solutions. The trend in MLCT energy is the same in CH_3CN.

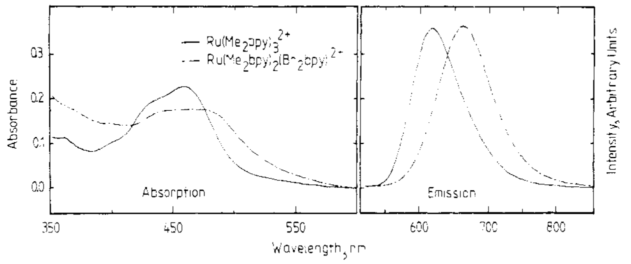

Figure 1. Absorption and emission spectra (excitation wavelength = 450 nm) of two complexes as their PF_6^- salts in deoxygenated CH_3CN solution at 25 °C. The relative emission intensities have been adjusted to clearly show the red shift of the emission maximum with incorporation of the Br-substituted ligand; cf. Table I.

Table II. Cyclic Voltammetry Data for Relevant Species[a]

	$E°'$(vs. Ag^+/Ag), V[b]			
species	3+/2+	2+/1+	1+/0	0/−1
Me_2bpy				−2.57
bpy				−2.51
$[Ru(bpy)_3]^{2+}$	0.97	−1.65	−1.86	−2.10
$[Ru(bpy)_2(Me_2bpy)]^{2+}$	0.93	−1.68	−1.88	−2.13
$[Ru(bpy)(Me_2bpy)_2]^{2+}$	0.90	−1.69	−1.90	−2.13
$[Ru(Me_2bpy)_3]^{2+}$	0.81	−1.76	−1.94	−2.18
$[Ru(bpy)_3]^{2+}$	0.97	−1.65	−1.86	−2.10
$[Ru(bpy)_2(Br_2bpy)]^{2+}$	1.02	*c*	*c*	*c*
$[Ru(bpy)(Br_2bpy)_2]^{2+}$	1.08	*c*	*c*	*c*
$[Ru(Br_2bpy)_3]^{2+}$	1.14	*c*	*c*	*c*
$[Ru(Me_2bpy)_3]^{2+}$	0.81	−1.76	−1.94	−2.18
$[Ru(Me_2bpy)_2(Br_2bpy)]^{2+}$	0.93	*c*	*c*	*c*
$[Ru(Me_2bpy)(Br_2bpy)_2]^{2+}$	1.03	*c*	*c*	*c*
$[Ru(Br_2bpy)_3]^{2+}$	1.14	*c*	*c*	*c*

[a] Data are for 10^{-3} M solutions of complex under N_2 in CH_3CN containing 0.1 M $[n\text{-}Bu_4N]BF_4$. [b] $E°'$ values represent the average of three successive measurements and are taken to be the average of the positions of the anodic and cathodic current peaks in cyclic voltammograms recorded at 50, 100, or 200 mV/s. [c] Irreversible reduction of the Br_2bpy species occurs. The first reduction peak in a 100 mV/s potential scan of the $[Ru(Br_2bpy)_3]^{2+}$ species is ~100 mV more positive than the first reduction peak of $[Ru(bpy)_3]^{2+}$.

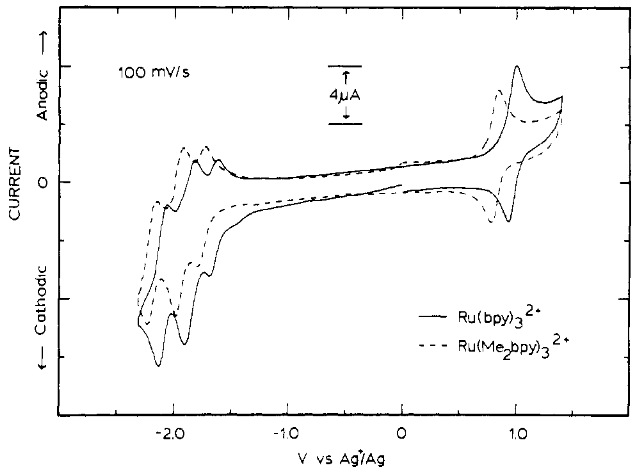

Figure 2. Cyclic voltammetry (Pt working electrode, 0.1 M $[n\text{-}Bu_4N]ClO_4$ in CH_3CN at 25 °C) of two complexes at ~1 mM to illustrate the effect of methyl substituents on the $E°'$s. The Ru(III/II) system, ~ +1.0 V, shifts ~0.2 V more negative upon introduction of Me groups; cf. Table II.

thesized are, upon photoexcitation, all emissive in fluid solution at 25 °C, as would be expected for the modest variations in the ligand system.[14] Likewise, the optical absorption spectra for all of the complexes are similar, showing a visible maximum in the vicinity of 450 nm with an absorptivity of ~1.5×10^4 M^{-1} cm^{-1}. The first optical absorption feature for the complexes is broad, and it is somewhat difficult to clearly discern the trends from substituent variation, but the optical emission data give significant insight into the nature of the substituent effect (Table I, Figure 1).

The optical emission spectra of the complexes are all fairly broad and featureless and are of approximately the same width. The absorption and emission spectra at 298 K for one pair of complexes are illustrated in Figure 1, and observed emission maxima for all complexes studied are given in Table I. In all cases the emission spectrum is independent of the excitation wavelength in the range ~500–240 nm. Since the spectra are all similar in shape and width, the emission maxima will be used to assess the effect of ligand variation on excited-state energies.

Consider first the series of bpy, Me_2bpy complexes. The Me_2bpy ligand is more difficult to reduce than bpy (Table II), and thus the $[Ru(Me_2bpy)_3]^{2+}$ species might be expected to exhibit a higher energy emission than $[Ru(bpy)_3]^{2+}$. However, the methyl substituents on the ligands *not* involved as the charge-acceptor ligand more than compensate for the extra difficulty in transferring substantial electron density to the remaining methylated charge-acceptor ligand. The MLCT emission maximum for $[Ru(Me_2bpy)_3]^{2+}$ is at *lower* energy than for $[Ru(bpy)_3]^{2+}$, because the electron-releasing groups on the two Me_2bpy ligands not involved as charge acceptors in the MLCT excited state affect the Ru d–π level. The Ru d–π level in the ground state of the Me_2bpy complex is expected to be less stable than in the bpy complex. In a series of homologous molecules, the $E°'$s for one-electron processes generally correlate well with the relative positions of the HOMO's and LUMO's. Thus, the relative one-electron d–π levels in the $[RuL_nL'_{3-n}]^{2+}$ species can be probed by electrochemistry, since the $Ru^{3+/2+}$ redox couple is reversible. Figure 2 shows a comparison of the cyclic voltammetry for $[Ru(bpy)_3]^{3+/2+}$ and $[Ru(Me_2bpy)_3]^{3+/2+}$, and data for these, and other, complexes are given in Table II. The difference in $E°'$s for the $Ru^{3+/2+}$ couples is ~0.2 V with the $(Me_2bpy)_3$ complex easier to oxidize than the $(bpy)_3$ complex. Inasmuch as the energy of an MLCT excited state is related to the ease with which the metal is oxidized and the ligand reduced, the more easily oxidized complex should have the lower energy MLCT state. Though it is evident from the cyclic voltammetry in Figure 2 that the LUMO

---

(13) (a) Lytle, F. E.; Hercules, D. M. *J. Am. Chem. Soc.* **1969**, *91*, 253. (b) Demas, J. N.; Adamson, A. W. *J. Am. Chem. Soc.* **1971**, *93*, 1800.

(14) Demas, J. N.; Harris, E. W.; McBride, R. P. *J. Am. Chem. Soc.* **1977**, *99*, 3547.

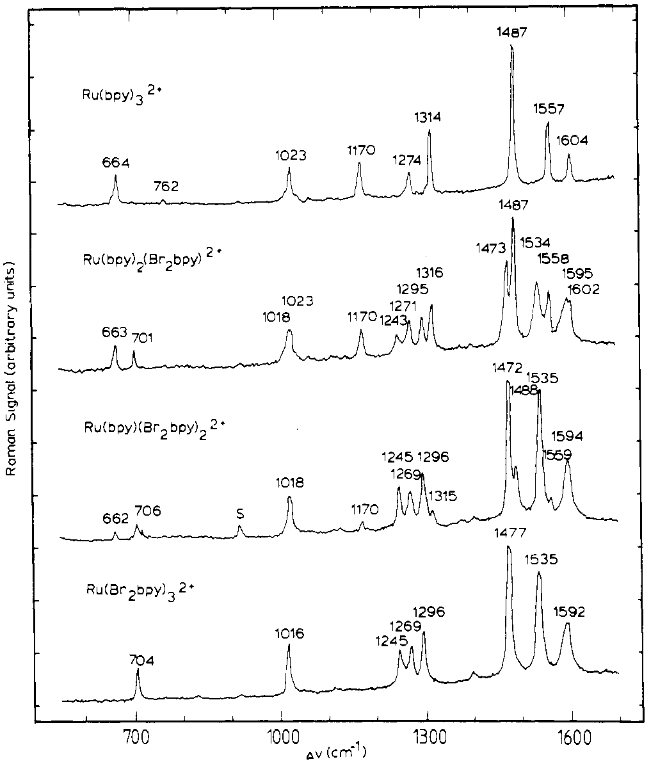

Figure 3. Ground-state Raman spectra (excited with a CW Ar ion laser tuned to 457.9 nm) of a series of complexes dissolved to ~1 mM in CH_3CN as their PF_6^- salts. The Raman frequencies are given above the peaks and are ±5 cm^{-1} in absolute position. The band marked S is due to solvent.

of $[Ru(Me_2bpy)_3]^{2+}$ is less stable than the LUMO of $[Ru(bpy)_3]^{2+}$, the d–π(HOMO) level of the $(Me_2bpy)_3$ complex is destabilized more.

Consider now a set of complexes such as the Br_2bpy, Me_2bpy series where the electron-withdrawing Br and -releasing Me substituents are involved. $[Ru(Me_2bpy)_2(Br_2bpy)]^{2+}$ has the lowest energy MLCT emission of all complexes studied. This is reasonable because the Me_2bpy ligands release electron density, destabilizating the d–π level, and Br_2bpy is more easily reduced than the other ligands. The point is that in assessing the effect of substituents on the energy of the lowest excited state, the substituents on ligands not involved as charge-acceptor ligands can be significant.

The emission spectra of the Re complexes $[fac\text{-}(CH_3CN)Re(CO)_3L]^+$ (L = Me_2bpy, bpy, Br_2bpy) (Table I) illustrate the "expected" substituent effect on the energy of the lowest MLCT excited state:[15] the energy is ordered according to the electron-releasing or -withdrawing power of the substituent. Note that the Re species also reveal the character of the ligand L as reflected by the CO stretching frequencies in CH_3CN: L = Me_2bpy, 2041 and 1935 cm^{-1}; L = Br_2bpy, 2044 and 1941 cm^{-1}. The Br_2bpy ligand withdraws electron density from the Re center, as reflected in the higher CO stretching frequencies. A homologous series involving the Ru(II) system is complicated by the presence of three similar charge-acceptor ligands. For example, $[Ru(bpy)_2L]^{2+}$ (L = Me_2bpy, bpy, Br_2bpy) does not always have a lowest Ru → L CT. When L = Me_2bpy, the lowest CT excited state is Ru → bpy; vide infra. Even in the series $[RuL_3]^{2+}$ (L = Me_2bpy, bpy, Br_2bpy), the CT energies do not have the same ordering as for the Re complexes. The $(Me_2bpy)_3$ species has a lower MLCT emission than the $(bpy)_3$ species, because the electron-releasing power of the two Me_2bpy ligands not involved as acceptors in the MLCT excited state lowers the energy and overcomes the extra difficulty in reducing the Me_2bpy ligand.

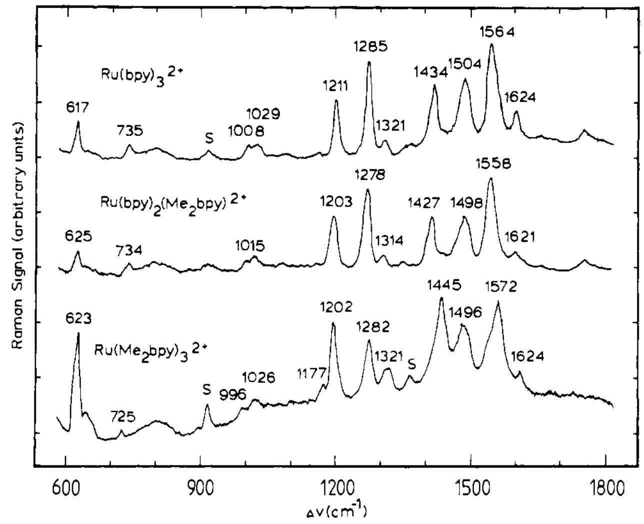

Figure 4. Excited-state Raman spectra of a series of complexes at ~1 mM in CH_3CN as their PF_6^- salts. Note that the spectrum of the mixed-ligand species, $[Ru(bpy)_2(Me_2bpy)]^{2+}$, is nearly identical with that of $[Ru(bpy)_3]^{2+}$. The excited state of the mixed-ligand complex is thus regarded as having an excited electron localized on one of the two bpy ligands. Absolute band positions are ±5 cm^{-1}.

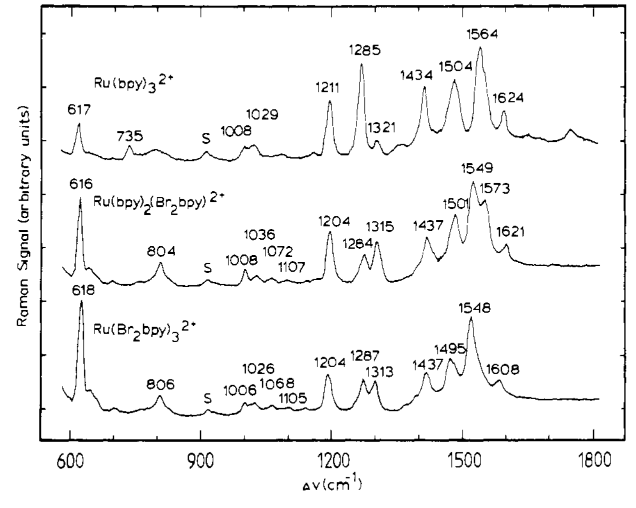

Figure 5. Excited-state Raman spectra of a series of complexes at ~1 mM in CH_3CN as their PF_6^- salts. The mixed-ligand complex exhibits a spectrum that most closely resembles that for $[Ru(Br_2bpy)_3]^{2+}$, consistent with an electron localized on the Br_2bpy ligand, but the feature noted at 1573 cm^{-1} in the mixed-ligand complex suggests that a fraction of the mixed-ligand excited states involves electron localization on the bpy ligand. Absolute band positions are ±5 cm^{-1}.

Raman Spectra of Ground- and Excited-State $[RuL_nL'_{3-n}]^{2+}$ Complexes. The variation in emission energies and electrochemical data for the $[RuL_nL'_{3-n}]^{2+}$ complexes (Tables I and II and Figures 1 and 2) can be rationalized by invoking various degrees of electron donation from the Me, H, and Br substituents on the bpy ligand. In the extreme of the complexes studied, $[Ru(Me_2bpy)_2(Br_2bpy)]^{2+}$, the electron-releasing Me-substituted ligands and electron-withdrawing Br-substituted ligand work together to give the lowest excited-state energy of all complexes studied. The assertion is that the electron is localized on the Br_2bpy ligand. We have established the validity of this and similar assertions by measuring the resonance Raman spectra of the excited $[RuL_nL'_{3-n}]^{2+}$ complexes. Tables III and IV and Figures 3–5 summarize the Raman spectroscopy data. The Raman spectra for the ground-state species have been measured by using 457.9-nm excitation, which is near the MLCT absorption maxima of the complexes. Strong Raman signals are obtained (Table III). In a series, such as the bpy, Br_2bpy set (Figure 3), the spectra of the mixed complexes show features clearly attributable to both

---

[15] (a) Ford, P.; Rudd, De F. P.; Gaunder, R.; Taube, H. *J. Am. Chem. Soc.* **1968**, *90*, 1187. (b) Wrighton, M. S.; Abrahamson, H. B.; Morse, D. K. *J. Am. Chem. Soc.* **1976**, *98*, 4105. (c) Giordano, P. J.; Wrighton, M. S. *Inorg. Chem.* **1977**, *16*, 160.

Table III. Ground-State Raman Frequencies ($\Delta\nu$, cm^{-1}) of Relevant Complexes Excited at 457.9 nm[a]

$[Ru(bpy)_3]^{2+}$	$[Ru(bpy)_2(Me_2bpy)]^{2+}$	$[Ru(bpy)(Me_2bpy)_2]^{2+}$	$[Ru(Me_2bpy)_3]^{2+}$
	560 (w)	565 (0.1)	576 (0.2)
664 (0.2)	663 (0.2)	661 (0.1)	
	739 (w)	742 (0.1)	742 (0.3)
762 (w)	762 (w)		
1023 (0.2)	1023 (0.2)	1023 (0.4)	1025 (0.4)
1170 (0.2)	1170 (0.2)	1171 (0.2)	
	1198 (w)	1201 (0.1)	1201 (0.2)
	1260 (0.1)	1260 (0.1)	1258 (0.3)
1274 (0.2)	1275 (0.2)	1272 (0.2)	1274 (0.3)
1314 (0.5)	1314 (0.4)	1320 (0.5)	1319 (0.6)
1487 (1.0)	1485 (1.0)	1487 (1.0)	1482 (1.0)
		1550 (0.5)	1550 (0.9)
1557 (0.4)	1557 (0.4)	1558 (0.5)	
1604 (0.2)	1602 (0.2)	1604 (0.3)	
		1619 (0.2)	1619 (0.2)

$[Ru(bpy)_3]^{2+}$	$[Ru(bpy)_2(Br_2bpy)]^{2+}$	$[Ru(bpy)(Br_2bpy)_2]^{2+}$	$[Ru(Br_2bpy)_3]^{2+}$
664 (0.2)	663 (0.2)	662 (w)	
	701 (0.1)	706 (0.1)	704 (0.2)
762 (w)			
	1018 (0.2)	1018 (0.3)	1016 (0.4)
1023 (0.2)	1023 (0.2)		
1170 (0.2)	1170 (0.2)	1170 (w)	
	1243 (0.1)	1245 (0.3)	1245 (0.3)
1274 (0.2)	1271 (0.3)	1269 (0.3)	1269 (0.3)
	1295 (0.3)	1296 (0.4)	1296 (0.4)
1314 (0.5)	1316 (0.4)	1315 (0.1)	
	1473 (0.7)	1472 (1.0)	1477 (1.0)
1487 (1.0)	1487 (1.0)	1488 (0.4)	
	1534 (0.5)	1536 (0.9)	1535 (0.8)
1557 (0.4)	1558 (0.4)	1559 (0.2)	
	1595 (0.3)	1594 (0.4)	1592 (0.4)
1604 (0.2)	1602 (0.3)		

$[Ru(Me_2bpy)_3]^{2+}$	$[Ru(Me_2bpy)_2(Br_2bpy)]^{2+}$	$[Ru(Me_2bpy)(Br_2bpy)_2]^{2+}$	$[Ru(Br_2bpy)_3]^{2+}$
576 (0.2)	567 (0.1)		
	707 (0.2)	707 (0.1)	704 (0.2)
742 (0.3)	743 (0.1)		
1025 (0.4)	1020 (0.4)	1020 (0.3)	1016 (0.4)
1201 (0.2)			
	1243 (0.3)	1247 (0.2)	1245 (0.3)
1258 (0.3)	1259 (0.2)		
1274 (0.3)	1273 (0.3)	1271 (0.2)	1269 (0.3)
	1303 (0.4)	1297 (0.3)	1296 (0.4)
1319 (0.6)	1324 (0.3)	1320 (0.1)	
	1473 (0.1)	1475 (0.9)	1477 (1.0)
1482 (1.0)	1486 (0.6)		
	1536 (0.8)	1539 (1.0)	1535 (0.8)
1550 (0.9)	1550 (0.5)		
	1595 (0.4)	1595 (0.5)	1592 (0.4)
1619 (0.2)	1616 (0.2)	1618 (0.1)	

[a] Numbers in parentheses represent uncorrected intensities reported relative to the most intense spectral feature. Bands with intensities significantly lower than 0.1 are indicated by "w".

Table IV. Excited-State Raman Frequencies ($\Delta\nu$, cm^{-1}) of Relevant Complexes at 354.7 nm[a]

$[Ru(bpy)_3]^{2+}$	$[Ru(bpy)_2(Me_2bpy)]^{2+}$	$[Ru(bpy)(Me_2bpy)_2]^{2+}$	$[Ru(Me_2bpy)_3]^{2+}$
617 (0.3)	625 (0.3)	631 (0.2)	623 (1.0)
735 (0.1)	734 (0.1)	743 (0.1)	725 (0.1)
1008 (0.1)	1015 (0.1)	1009 (0.2)	996 (w)
1029 (0.1)		1029 (0.2)	1026 (0.1)
			1177 (0.1)
1211 (0.5)	1203 (0.6)	1205 (0.7)	1202 (0.4)
1285 (0.9)	1278 (0.9)	1279 (0.9)	1282 (0.6)
1321 (0.1)	1314 (0.1)	1318 (0.2)	1321 (0.2)
1434 (0.6)	1427 (0.5)	1422 (0.8)	
		1445 (0.6)	1445 (0.9)
1504 (0.7)	1498 (0.5)	1493 (0.7)	1496 (0.6)
1564 (1.0)	1558 (1.0)	1550 (1.0)	1572 (0.9)
1624 (0.3)	1621 (0.2)	1621 (0.2)	1624 (0.2)

$[Ru(bpy)_3]^{2+}$	$[Ru(bpy)_2(Br_2bpy)]^{2+}$	$[Ru(bpy)(Br_2bpy)_2]^{2+}$	$[Ru(Br_2bpy)_3]^{2+}$
617 (0.3)	616 (1.0)	624 (w)	618 (1.0)
735 (0.1)			
	804 (0.3)	806 (0.1)	806 (0.2)
1008 (0.1)	1008 (0.2)	1008 (0.1)	1006 (0.1)
1029 (0.1)	1036 (0.1)	1028 (0.1)	1026 (0.1)
	1072 (w)	1072 (w)	1068 (w)
	1107 (w)	1103 (w)	1105 (w)
1211 (0.5)	1204 (0.6)	1200 (0.5)	1204 (0.3)
1285 (0.9)	1284 (0.3)	1279 (0.3)	1287 (0.3)
1321 (0.1)	1315 (0.4)	1311 (0.4)	1313 (0.3)
1434 (0.6)	1437 (0.4)	1437 (0.6)	1437 (0.3)
1504 (0.7)	1501 (0.7)	1501 (0.5)	1495 (0.4)
	1549 (1.0)	1549 (1.0)	1548 (0.8)
1564 (1.0)	1573 (0.8)		
1624 (0.3)	1621 (0.3)	1602 (0.1)	1608 (0.2)

$[Ru(Me_2bpy)_3]^{2+}$	$[Ru(Me_2bpy)_2(Br_2bpy)]^{2+}$	$[Ru(Me_2bpy)(Br_2bpy)_2]^{2+}$	$[Ru(Br_2bpy)_3]^{2+}$
623 (1.0)	624 (0.1)	628 (0.2)	618 (1.0)
725 (0.1)			
	810 (0.2)	810 (0.1)	806 (0.2)
996 (w)	1006 (0.2)	1010 (0.1)	1006 (0.1)
1026 (0.1)	1032 (w)	1032 (0.1)	1026 (0.1)
	1068 (w)	1069 (w)	1068 (w)
	1105 (w)	1104 (w)	1105 (w)
1177 (0.1)			
1202 (0.4)	1201 (0.6)	1200 (0.4)	1204 (0.3)
1282 (0.6)	1282 (0.4)	1277 (0.4)	1287 (0.3)
1321 (0.2)	1311 (0.4)	1312 (0.4)	1313 (0.3)
	1426 (0.5)	1426 (0.5)	1437 (0.3)
1445 (0.9)			
1496 (0.6)	1491 (0.5)	1491 (0.6)	1495 (0.4)
	1538 (1.0)	1542 (1.0)	1548 (0.8)
1572 (0.9)		1595 (0.3)	
1624 (0.2)	1625 (0.1)	1621 (0.2)	1608 (0.2)

[a] Numbers in parentheses represent uncorrected intensities reported relative to the most intense spectral feature. Bands with intensities significantly lower than 0.1 are indicated by "w".

ligands. In Figure 3, for example, the features at 664, 1170, and 1314 cm^{-1} are characteristic of the bpy ligand (not present in the spectrum of $[Ru(Br_2bpy)_3]^{2+}$), while the features at 704, 1245, and 1296 cm^{-1} are characteristic of the Br_2bpy ligand (not present in the spectrum of $[Ru(bpy)_3]^{2+}$). In the mixed complexes, all of the features are observed and variations in the relative intensities accord well with the number of one ligand or the other; compare the 664–704-cm^{-1} features in the four spectra shown in Figure 3. The ground-state Raman spectra of the other sets of complexes are similarly clear: features characteristic of both ligands in mixed complexes (Table III) are prominent in the ground-state Raman spectra.

The Raman spectra of the excited $[RuL_nL'_{3-n}]^{2+}$ species (Table IV) have been obtained by monitoring the Raman scattering from the trailing portion of a 354.7-nm laser pulse of ~18 ns, the leading portion of which completely depopulates the ground state. The 354.7-nm excitation is close to a strong absorption of bpy^-, and intense Raman signals can be observed for the CT state of $[RuL_nL'_{3-n}]^{2+}$ that are similar to those expected for L^- or L'^-. The $[RuL_3]^{2+}$ (L = bpy, Me_2bpy, Br_2bpy) complexes all give strong, characteristic excited-state Raman spectra that provide a basis for assigning the spectra of mixed-ligand complexes. Moreover, we find that the excited-state Raman spectra of the $[\textit{fac}\text{-}(CH_3CN)Re(CO)_3L]^+$ complexes are quite similar to those for $[RuL_3]^{2+}$, in accord with excited states that can be regarded as complexes of L^-. It has been previously shown that the excited-state Raman spectrum of $ClRe(CO)_3bpy$ is nearly the same as that for $[Ru(bpy)_3]^{2+}$.[7e] The excited-state spectra are dominated by resonance Raman bands associated with the ligand on which the excited electron becomes localized. The "unreduced" ligands show relatively weak Raman bands, and features of the unreduced ligands are not typically observed, as found previously.[7e] We have

Table V. Conclusions Regarding the Ligand of Localization of the Excited Electron in $[\mathrm{RuL}_n\mathrm{L'}_{3-n}]^{2+}$ Complexes

	ligand of localization	
complex	from excited-state Raman	from emission energy
$[\mathrm{Ru(bpy)(Me_2bpy)_2}]^{2+}$	mixed	bpy
$[\mathrm{Ru(bpy)_2(Me_2bpy)}]^{2+}$	bpy	bpy
$[\mathrm{Ru(bpy)_2(Br_2bpy)}]^{2+}$	mixed	$\mathrm{Br_2bpy}$
$[\mathrm{Ru(bpy)(Br_2bpy)_2}]^{2+}$	$\mathrm{Br_2bpy}$	$\mathrm{Br_2bpy}$
$[\mathrm{Ru(Me_2bpy)_2(Br_2bpy)}]^{2+}$	$\mathrm{Br_2bpy}$	$\mathrm{Br_2bpy}$
$[\mathrm{Ru(Me_2bpy)(Br_2bpy)_2}]^{2+}$	$\mathrm{Br_2bpy}$	$\mathrm{Br_2bpy}$

assumed that 345.7 nm will give resonance Raman spectra for all ligands used. The absorption spectra of the various L^- species are expected to be quite similar, and the intense excited-state Raman spectra appear to be consistent with expectation.

Excited-state Raman spectra of the mixed-ligand complexes are most interesting. Figure 4 shows a comparison of the excited-state Raman spectra of $[\mathrm{Ru(bpy)_3}]^{2+}$, $[\mathrm{Ru(bpy)_2(Me_2bpy)}]^{2+}$, and $[\mathrm{Ru(Me_2bpy)_3}]^{2+}$. The spectra of excited $[\mathrm{Ru(bpy)_3}]^{2+}$ and $[\mathrm{Ru(Me_2bpy)_3}]^{2+}$ are different; note particularly the characteristic intensities and frequencies of the signals in the 1100–1700-cm^{-1} region. *Importantly, the spectrum of excited* $[\mathrm{Ru(bpy)_2(Me_2bpy)}]^{2+}$ *is nearly the same as that for* $[\mathrm{Ru(bpy)_3}]^{2+}$. For the $[\mathrm{Ru(bpy)_2(Me_2bpy)}]^{2+}$ complex, the ground-state spectrum (Table IV) clearly shows signals due to bpy (1170 cm^{-1}) and $\mathrm{Me_2bpy}$ (1260 cm^{-1}). The excited-state spectrum of $[\mathrm{Ru(bpy)_2(Me_2bpy)}]^{2+}$ is consistent with the conclusion that the relaxed excited state is best viewed as one with the excited electron localized on one of the bpy ligands, $[\mathrm{Ru^{III}(bpy^-)(bpy)(Me_2bpy)}]^{2+}$. This is the same conclusion that can be drawn from the *red* shift in the emission maximum of $[\mathrm{Ru(bpy)_2(Me_2bpy)}]^{2+}$ compared to that of $[\mathrm{Ru(bpy)_3}]^{2+}$ (Table I).

Figure 5 shows the excited-state Raman spectra for $[\mathrm{Ru(bpy)_3}]^{2+}$, $[\mathrm{Ru(bpy)_2(Br_2bpy)}]^{2+}$, and $[\mathrm{Ru(Br_2bpy)_3}]^{2+}$. In this series the mixed-ligand complex gives a spectrum that is very similar to that of $[\mathrm{Ru(Br_2bpy)_3}]^{2+}$; in this case the 1000–1100-cm^{-1} region and the 1200–1620-cm^{-1} region are compelling. The conclusion is that the relaxed CT state of $[\mathrm{Ru(bpy)_2(Br_2bpy)}]^{2+}$ has the excited electron localized on the $\mathrm{Br_2bpy}$ ligand, again a conclusion that can be drawn from the emission energies of the complexes in the series.

Table IV includes excited-state Raman data for all complexes. Generally, it can be concluded that the excited electron is localized on the most easily reduced ligand. However, two of the mixed-ligand complexes show evidence of a mixture of excited states. In the excited-state Raman spectrum of $[\mathrm{Ru(bpy)_2(Br_2bpy)}]^{2+}$, there is a 1573-cm^{-1} shoulder on the 1549-cm^{-1} feature (Figure 5). The 1573-cm^{-1} peak, near a strong feature in the excited-state spectrum of $[\mathrm{Ru(bpy)_3}]^{2+}$, suggests that a small fraction of the excited species has the excited electron localized on a bpy ligand. Similar evidence for a mixture of excited species exists for the $[\mathrm{Ru(bpy)(Me_2bpy)_2}]^{2+}$ species (Table IV). It should be noted that our data do not unambiguously rule out a single excited-state species that has the excited electron density delocalized over the various ligands. However, the mixture of excited species is not unreasonable: the emission energies in both series of complexes are different by no more than 1000 cm^{-1}. Thus, the two possible types of excited states differ by only a small amount in energy. Additionally, the 354.7-nm excitation likely produces a mixture of the two possible excited species that may be slow to reach the lowest MLCT excited state compared to the time of the probe. The excitation/interrogration pulse is only ~18 ns. The excited-state spectra as a function of time after the excitation pulse cannot be obtained with the equipment available, but work toward resolving the distribution of excited species as a function of time is under way in these laboratories. Table V summarizes the conclusions concerning excited-electron localization in the $[\mathrm{RuL}_n\mathrm{L'}_{3-n}]^{2+}$ complexes studied.

Acknowledgment. We thank the National Science Foundation for support of this research by a grant to M.S.W. The excited-state Raman spectroscopy was carried out in the NSF Regional Laser Facility at MIT. We are grateful for the availability of these facilities.

Note Added in Proof. We wish to note the related article, which appeared while ours was in press: McClanahan, S. F.; Dallinger, R. F.; Holler, F. J.; Kincaid, J. R. *J. Am. Chem. Soc.* **1985**, *107*, 4853.

Registry No. $\mathrm{Br_2bpy}$, 18511-71-2; $\mathrm{Ru(4,4'\text{-}Me_2bpy)_2Cl_2}$, 68510-55-4; $\mathrm{Ru(4,4'\text{-}Br_2bpy)_2Cl_2}$, 99666-63-4; $[\mathrm{Ru(bpy)_2(Me_2bpy)}][\mathrm{PF_6}]_2$, 99685-99-1; $[\mathrm{Ru(bpy)_2(Br_2bpy)}][\mathrm{PF_6}]_2$, 99666-65-6; $[\mathrm{Ru(Me_2bpy)_2(bpy)}][\mathrm{PF_6}]_2$, 99666-66-7; $[\mathrm{Ru(Me_2bpy)_2(Br_2bpy)}][\mathrm{PF_6}]_2$, 99666-68-9; $[\mathrm{Ru(Br_2bpy)_2(bpy)}][\mathrm{PF_6}]_2$, 99666-70-3; $[\mathrm{Ru(Br_2bpy)_2(Me_2bpy)}][\mathrm{PF_6}]_2$, 99666-72-5; $[\mathrm{Ru(bpy)_3}][\mathrm{PF_6}]_2$, 60804-74-2; $[\mathrm{Ru(Me_2bpy)_3}][\mathrm{PF_6}]_2$, 83605-44-1; $[\mathrm{Ru(Br_2bpy)_3}][\mathrm{PF_6}]_2$, 99666-73-6; $\mathrm{Ru(bpy)_2Cl_2}$, 15746-57-3; [*fac*-$\mathrm{(CH_3CN)Re(CO)_3(bpy)}][\mathrm{CF_3SO_3}]$, 75699-14-8; [*fac*-$\mathrm{(CH_3CN)Re(CO)_3(Me_2bpy)}][\mathrm{CF_3SO_3}]$, 99666-75-8; [*fac*-$\mathrm{(CH_3CN)Re(CO)_3(Br_2bpy)}][\mathrm{CF_3SO_3}]$, 99666-77-0; $\mathrm{ClRe(CO)_3(bpy)}$, 55658-96-3; $\mathrm{ClRe(CO)_3(Me_2bpy)}$, 99666-78-1; $\mathrm{ClRe(CO)_3(Br_2bpy)}$, 99666-79-2; $[\mathrm{Ru(bpy)_3}]^{3+}$, 18955-01-6; $[\mathrm{Ru(bpy)_2(Me_2bpy)}]^{3+}$, 99666-80-5; $[\mathrm{Ru(bpy)(Me_2bpy)_2}]^{3+}$, 99666-81-6; $[\mathrm{Ru(Me_2bpy)_3}]^{3+}$, 47837-95-6; $[\mathrm{Ru(bpy)_2(Br_2bpy)}]^{3+}$, 99666-82-7; $[\mathrm{Ru(bpy)(Br_2bpy)_2}]^{3+}$, 99666-83-8; $[\mathrm{Ru(Br_2bpy)_3}]^{3+}$, 99666-84-9; $[\mathrm{Ru(Me_2bpy)_2(Br_2bpy)}]^{3+}$, 99666-85-0; $[\mathrm{Ru(Me_2bpy)(Br_2bpy)_2}]^{3+}$, 99666-86-1; $[\mathrm{Ru(bpy)_3}]^{+}$, 56977-24-3; $[\mathrm{Ru(bpy)_2(Me_2bpy)}]^{+}$, 99666-87-2; $[\mathrm{Ru(bpy)(Me_2bpy)_2}]^{+}$, 99666-88-3; $[\mathrm{Ru(Me_2bpy)_3}]^{+}$, 65605-26-7; $\mathrm{Ru(bpy)_3}$, 74391-32-5; $\mathrm{Ru(bpy)_2(Me_2bpy)}$, 99666-89-4; $\mathrm{Ru(bpy)(Me_2bpy)_2}$, 99666-90-7; $\mathrm{Ru(Me_2bpy)_3}$, 83605-52-1; $\mathrm{Me_2bpy^-}$, 98789-73-2; $\mathrm{bpy^-}$, 34475-06-4; $[\mathrm{Ru(bpy)_3}]^-$, 56977-23-2; $[\mathrm{Ru(bpy)_2(Me_2bpy)}]^-$, 99666-91-8; $[\mathrm{Ru(bpy)(Me_2bpy)_2}]^-$, 99666-92-9; $[\mathrm{Ru(Me_2bpy)_3}]^-$, 83605-53-2; $\mathrm{Me_2bpy}$, 1134-35-6; bpy, 366-18-7.